Virtual rolling automation and setup calculations for six stands FEM finishing mill

Virtual rolling automation and setup calculations for six stands FEM finishing mill

J Ilmola*, O Seppälä, A Pohjonen and J Larkiola
Materials and Mechanical Engineering, Centre for Advanced Steels Research, University of Oulu, University of Oulu, P.O. Box 4200, FI-90014, Finland
* Corresponding author, E-mail: joonas.ilmola@oulu.fi

Abstract. Digitalization is becoming increasingly common in the steel industry. Formerly developed models of individual phenomenon or separate sub-processes are being further developed into wider complexes where multiple models are coupled together. Virtual rolling automation, which can be used to control a finite-element rolling model, is a new element in these complexes. The automation enables to model the variations caused by the process adjustment. It must be taken in the account that neither the model nor the industrial process are ideal, but there are limitations in the attainable accuracy in both cases. Inclusion of the new automation control in the FE-model introduces new requirements: the setup calculations for all six rolling stands and the automation logic adjustments must perform within the model. The focus of the current article is prediction of the roll force and the virtual rolling automation of six stand finishing mill.

1. Introduction

Hot rolling is a metal forming process in which a steel slab is rolled through the revolving rolls producing thickness reduction in the slab. A steel strip is produced by several hot rolling passes. Hot rolling process is widely applied in steel industrial due to high productivity, modifiability, automatization and reliable mechanics. Virtual rolling automation and setup calculations for six stands FEM finishing mill in hot rolling process are developed

Terms digital twin and virtual rolling appear commonly in discussion of modelling steel rolling processes. These are not new terms but meaning of those has changed over time while models and computers have developed. Individual phenomena regarding the steel rolling and metallurgy have been studied and theories developed over a century [1–8]. These theories have been coupled using different modelling methods to understand mutual effect of certain phenomena into properties of steel. The latest models also consider the response of the final product to the changes in the manufacturing process and rolling automation [9]. This approach enables to take the manufacturing conditions into account. This kind of fundamental modelling minimizes the number of assumptions and makes modelled rolling process interactive. Modern rolling model must be assimilable to the industrial process. This means thoroughly modelled mechanical and metallurgical phenomena, setup calculations and interactive virtual rolling automation (VRA). In this article, the full model is realized by utilizing Finite Element Method (FEM)-model of six stands finishing mill.

Setup calculations are required for accurate roll gap control in FEM as well as to predefine rolling speeds. Setup calculations are based on contact pressure between the work roll (WR) and the steel strip. Contact pressure on contact arc is utilized to define roll force, to calculate the WR surface displacements (flattening) and the rolling stand elongation. Material flow and strip tensioning must be controlled in a single FEM-model of six stand finishing mill. This presumes VRA implemented into FEM. By coupling

the setup calculations and the VRA the model is equivalent to the industrial hot rolling process and effect of the controlled manufacturing process is integrated into the model.

Nomenclature

p	contact pressure	Δt	draft
τ	friction shear stress	f	forward slip
Y_s	yield stress on uniaxial compression	V_0	threading velocity of strip
$2k$	yield stress in plane-strain	V_{ex}	strip exit velocity
k	yield stress in pure shear	V_r	circumferential velocity of work roll
R	undeformed radius of work roll	V_ω	angular velocity of work roll
R'	deformed circular radius of work roll	$\dot{\varepsilon}$	strain rate
μ	friction coefficient	ε	true strain
α	contact angle of entrance	a_{1-9}	Hensel-Spittel fitting parameters
t_{en}	strip entry thickness contact pressure	p_{en}	entry plane contact pressure
t_{ex}	strip exit thickness	p_{ex}	exit plane contact pressure
β	neutral angle	$tens_{en}$	entry tension
Y	strip thickness at neutral angle	$tens_{ex}$	exit tension
E	elastic modulus of work roll	h	strip thickness at θ
ν	poisson constant	β	neutral angle
w	strip width	P	roll force
r	reduction	T	strip temperature
A	Total area of radiating surface	f_E	emissivity
C	specific heat	V	workpiece volume
H_c	work roll heat-conduction factor	ρ	density
T_{roll}	temperature of work roll	S	Stefan-Boltzmann factor
T_a	ambient temperature	N	rolling speed [rev/min]

2. FEM-model

Finite element (FE) model of finishing mill is introduced by authors in previous articles [10,11]. Model principles and mechanics are based on these publications. Software used for the FE-modeling is Abaqus™. FEM as a modelling method enables take into account the realistic mechanical boundary conditions. Strip entry and exit angle in proportion to roll gap changes continuously due to looper tensioning and variations in process. Moreover, metallurgical phenomena between individual passes may influence the flow stress. These changes lead to transient rolling process which requires continuous reactions from automation system to keep the process stable. All these small variations in process due to automation adjustments have been usually ignored in earlier single pass steady state rolling models. Sum of all these minor boundary condition plays an important role in many metallurgical phenomena which are time-depended and sensitive to strain, temperature and stress state. Four stands of the FE-model of finishing mill are shown in figure 1.

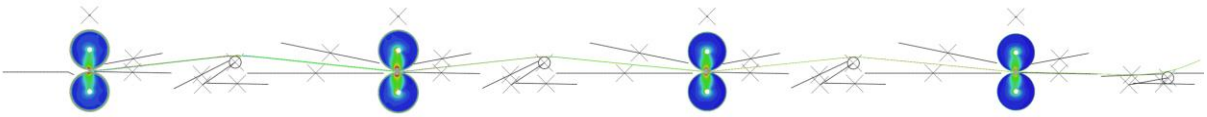

Figure 1. FE-model of finishing mill.

Simulation run of this FE finishing mill mimics real rolling process. Industrial rolling process requires precalculated setup values before actual rolling. Setup calculations predict initial rolling parameters for the automation system and enable stable rolling process. For the multi-stand rolling process the value of the setup calculation is emphasized. At the strip threading the roll gap clearance need to be preadjusted

considering the WR flattening and stand elongations. To predict these parameters precisely the roll force must be calculated. Accurately predicted gap clearance produces correct exit thickness and velocity of the strip. It is very important that predicted parameters are realized at former stands so that pre-adjustments for the subsequent stands are feasible. Otherwise, the automation system must make corrections to stable material flow between the stands. This is carried out by controlling the loopers and the rolling speed of the previous rolling stands. In any case, the rolling process cannot be completed only using setup parameters. After the threading, sensors measure data for the automation system and the rolling automation starts to adjust the process according to this measured data. Now the predicted parameters are replaced by measured ones. The better the set values, the less adjustment is required by the rolling automation.

Six stand FEM-model of finishing mill is developed to mimic real rolling process. Setup calculations are utilized to pre-adjust the FEM finishing mill and after the rolling process has started the VRA takes over the control and uses the measured sensor data from FEM-model. After the 2nd stand threading the material flow and strip tensioning between stands need to be controlled. Material flow is controlled regulating the rolling speed of a former stand. Looper roll has a reference point where VRA aims by changing the rolling speed of the previous stand (figure 2). Looper torque is adjusted according to torque arm developed between horizontal difference of torque motor shaft and looper roll.

The VRA is implemented into the FE-model using VUAMP-subroutine. VUAMP is able to read sensor data from the FE-model and it is possible control different loads and boundary conditions utilizing the so called user defined amplitudes within the applied Abaqus software. VUAMP includes setup calculations and operates rolling process with predicted parameters until sensor data is received. Calculations for strip tensioning by loopers and automation logic is explained by author's previous article in Ref. [10].

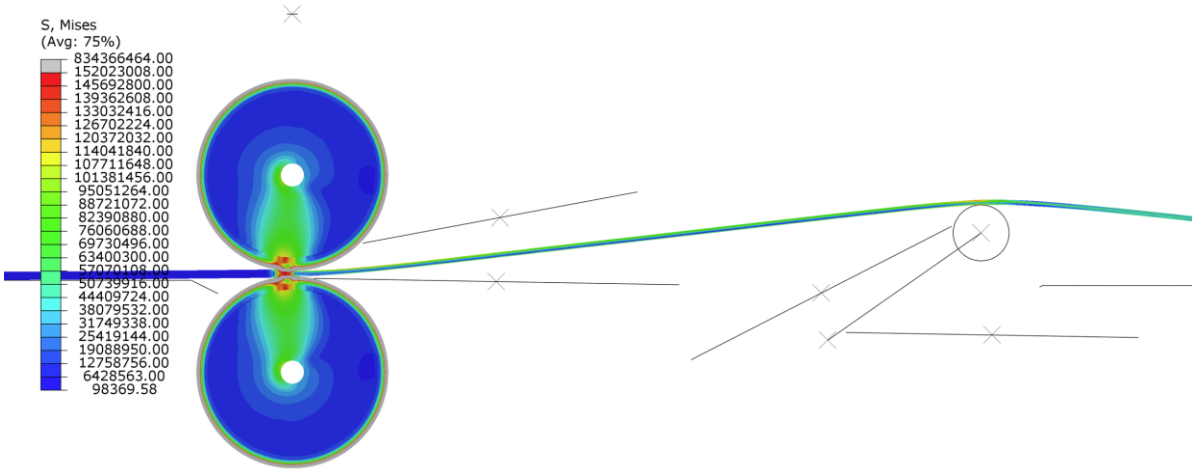

Figure 2. First rolling stand and looper of the FE-model.

3. ARCPRESS – Setup calculations

Modern models predicting roll force in cold and hot rolling processes are mainly deduced from Karman [3] and Orowan [5] differential equations. Horizontal stress in the roll bite is assumed differently in these equations. Karman assumes slippage between WR and the rolled material whereas Orowan does not assume slippage, however it contains criteria for determining slipping and sticking. Later SIMS [6] deduced analytical solution of Orowan equation assuming pure sticking friction conditions in hot rolling. SIMS equation was suitable for online process adjustment due to short computing time. Afterwards computing power was not the limiting factor and more complex methods can be solved online. Alexander [2] presented an extensive numerical solution to von Karman's equation. Alexander considered slipping and sticking friction regions. Alexander and more recently Chen [12] presented model for calculating contact pressure p over the contact arc between WR and the material by the angular

coordinate θ. Chen derivate the improved Karman equation by constituting the vertical and horizontal force equilibrium equation of the infinitesimal body. By dividing the contact arc into slipping and sticking friction zones and substituting these contact conditions again in equilibrium equations, yields the equations (2, 3, 6). Obtained differential equations (1, 5) are:
When Coulomb slipping friction: $\mu \cdot p < k$: $\tau = \pm\mu \cdot p$,

$$\frac{ds}{d\theta} = g_1(\theta)p + g_2(\theta) \tag{1}$$

where:

$$g_1(\theta) = \frac{\mp\mu\, sec\,\theta(2R' + hsec\,\theta)}{(1 \pm \mu\, tan\,\theta)h} \tag{2}$$

$$g_2(\theta) = \frac{h\frac{d(2k)}{d\theta} + 2R'(2k)sin\theta}{(1 \pm \mu\, tan\,\theta)h} \tag{3}$$

Equation (4) presents strip thickness at θ.

$$h = t_{ex} + 2R'(1 - \cos\theta) \tag{4}$$

The plus sign is used for the backward slip zone and minus sign for the forward slip zone.

And when sticking friction: $\mu \cdot p \geq k$: $\tau = \pm k$

$$\frac{ds}{d\theta} = g_3(\theta) \tag{5}$$

where:

$$g_3(\theta) = 2k\left(\frac{2R'}{h}sin\theta\left(1 \mp \frac{1}{2}tan\theta\right) \mp \left(\frac{R'}{h}cos\theta + \frac{1}{2}sec^2\theta\right)\right) + \left(1 \mp \frac{1}{2}tan\theta\right)\frac{d(2k)}{d\theta} \tag{6}$$

Freshwater [13,14] enhanced Alexander's numerical solution for calculating roll pressure, roll force and roll torque. Freshwater presented modified von Karman solution and inhomogeneous Orowan solution. In a modified von Karman approach the derivative of the yield stress function $2k(\theta)$ is eliminated and replaced with more realistic constitutive behaviour by inhomogeneous Orowan solution considering the stress distribution at any point in cross-section to depend upon local values of yield stress and surface friction in cylinder coordinates. In 2014 Chen presented improved von Karman equation which divides contact arc in slipping and sticking friction section using $g_{1,2,3}(\theta)$ functions similar than Alexander [2,12]. Setup calculations in this paper utilize equations presented in works of Chen and Alexander.
ARCPRESS setup calculations are calculated consecutively for each stand in the finishing mill. In the finishing mill consecutive passes occur in relatively short time and many parameters from previous pass have a clear effect on the next rolling pass. Parameters like strip exit velocity and exit thickness can be calculated instantly after the pass whereas some parameters need to be calculated right before the next rolling pass, since the interpass time has a significant effect on them. Such parameters are e.g. temperature, flow stress, recovery phenomena and cumulative metallurgical strain. Metallurgical phenomena are not presented in this paper. Fundamental roll bite parameters (figure 3) are required to define forward slip, angular velocity of the WR and the strip exit velocity. Contact angle of entrance and neutral angle are defined in following equations (7 and 8), respectively:

$$\alpha = acos\left(-0.5\frac{t_{en-}t_{ex}}{R'} + 1.0\right) \tag{7}$$

$$\beta = sin^{-1}\left(\frac{1}{2}\left(sin\,\alpha - \frac{1-cos\,\alpha}{\mu}\right)\right) \tag{8}$$

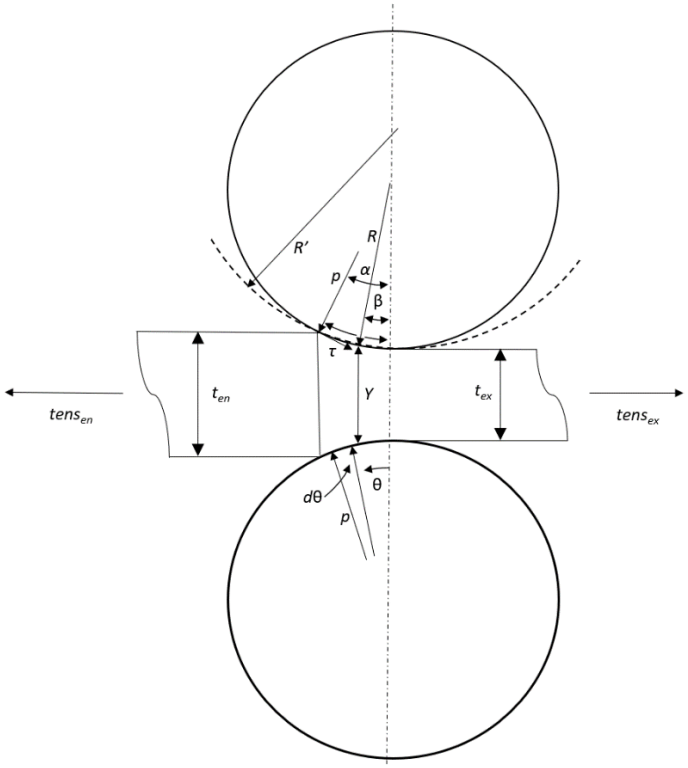

Figure 3. Schematic illustration of rolling parameters.

Deformed circular roll radius is calculated by iterative method. Hitchcock's [1] equation (9) of deformed work roll radius is used:

$$\frac{R'}{R} = 1 + \frac{16 \cdot (1-\upsilon^2)}{\pi \cdot E} \cdot \frac{P}{w \cdot \Delta t} \tag{9}$$

Equations for circumferential (10) and angular (11) velocities of WR are as follows:

$$V_r = \frac{V_{ex}}{f_i + 1}, \qquad V_\omega = \frac{V_{ex}}{(f_i + 1) \cdot R} \tag{10, 11}$$

where forward slip, strip exit velocity and neutral thickness are depicted with equations (12, 13, 14) below:

$$f_i = \frac{Y}{t_{ex}} cos\,\beta \tag{12}$$

$$V_{ex} = V_0 \cdot \frac{t_{en}}{t_{ex}} \quad (plane\ strain) \tag{13}$$

$$Y = t_{\mathrm{ex}} + 2 \cdot R' \cdot (1 - cos\,\beta) \tag{14}$$

Neutral angle is calculated with equation (8) on the first iteration loop when rolling pressure distribution are not calculated. When contact pressure distributions have been calculated first time the neutral angle

location is defined in intersection point of forward and backward zone pressure distributions and this value is used on the next computing loop. Synchronously all the other parameters are updated.

3.1. Constitutive and temperature models

Flow stress $2k$ in equation (16) in constitutive model is defined using Hensel-Spittel (HS) [15] equation (15). Experimental stress-strain behaviour of selected steel was tested with thermo-mechanical simulator Gleeble™ 3800. Specimens were tested in hot rolling temperatures 800°C - 1200°C with several strain rates 0.01 – 100 1/s using constant true strain 0.8. Fitting parameters a_{1-9} in table 1 were find using a sum of differences minimization method. The same method is utilized earlier by authors in Ref. [16]. Gleeble hot compression stands upon uniaxial stress state in compression and thus conversion to plane-strain stress state is required in modelling of hot rolling. Referring Huber-Mises theory the Y_s need to be corrected with constant factor of $\frac{2}{\sqrt{3}}$ [5]. In the FE-model flow stress model is implemented using VUHARD-subroutine in Abaqus. Experimental strain-stress curves and fitted curves are depicted in figure 4.

$$Y_s = a_1 \cdot \varepsilon^{a_2} \cdot exp(a_5\varepsilon) \cdot \dot{\varepsilon}^{a_3} \cdot exp(-a_4 T) \cdot (1+\varepsilon)^{a_6 T} \cdot \varepsilon^{a_7 \cdot T} \cdot T^{a_8} \cdot exp\left(\frac{a_9}{\varepsilon}\right) \quad (15)$$

$$2k = \frac{2}{\sqrt{3}} Y_s \quad (16)$$

Table 1. Fitting parameters for Hensel-Spittel equation.

a_1	a_2	a_3	a_4	a_5	a_6	a_7	a_8	a_9
3644.7	0.42837	0.13371	0.00236	-0.81999	0.0001	-6.45e-5	-0.03239	-1e-7

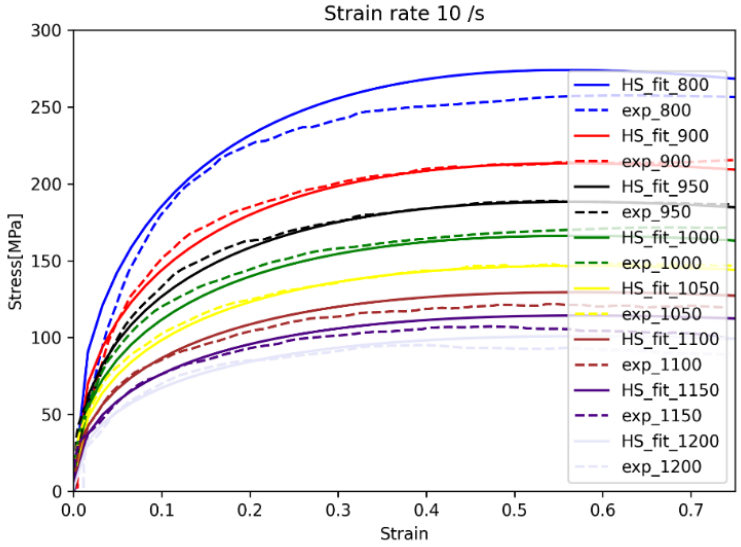

Figure 4. Comparison of experimental strain-stress curves (exp) to fitted curves (HS_fit).

where equation (17) of strain rate according to SIMS in [6] is:

$$\dot{\varepsilon} = \frac{2 \cdot V_r \cdot sin\,\beta}{t_{ex} + 2 \cdot R' \cdot (1 - cos\,\beta)} \quad (17)$$

Temperature is a crucial factor in calculation of flow stress. At typical finishing mill temperatures 1050°C - 800°C even small differences in temperature may affect significantly in flow stress. Plastic work due to deformation in roll bite generates heat and it is considered by equation (18) in [17]:

$$\Delta T_{def} = \frac{2k}{\rho c} \cdot ln\left(\frac{1}{1-r}\right) \tag{18}$$

Strip also loose heat in contact with WR. Temperature decreases in the strip due to conductivity between the WR and the strip can be obtained by equation (19), referring [17]:

$$\Delta T_{cond} = 60 \cdot H_c \cdot \sqrt{\frac{r}{t_{en} R'}} \cdot (T - T_{roll}) \cdot [(1-r) \cdot \pi \rho C N]^{-1} \tag{19}$$

During interpass sections strip loose heat due to thermal radiation and convection [17]. This is calculated using equation (20):

$$\frac{\mathrm{dT}}{\mathrm{dt}} = -A f_E S (CV\rho)^{-1} (T^4 - T_a^4) \tag{20}$$

3.2. Calculation of roll force

Differential equations (22-24) can be gathered into single stress balanced differential equation (21):

$$\frac{dp}{d\theta} = G_1(\theta)p + G_2(\theta) + G_3(\theta) \tag{21}$$

where function $g_{1-2}(\theta)$ are used on account of slipping friction conditions and function $g_3(\theta)$ on sticking friction conditions.

$$G_1(\theta) = \begin{cases} g_1(\theta) & ,\mu \cdot p < k \\ 0 & ,\mu \cdot p \geq k \end{cases}, \tag{22}$$

$$G_2(\theta) = \begin{cases} g_2(\theta) & ,\mu \cdot p < k \\ 0 & ,\mu \cdot p \geq k \end{cases}, \tag{23}$$

$$G_3(\theta) = \begin{cases} 0 & ,\mu \cdot p < k \\ g_3(\theta) & ,\mu \cdot p \geq k \end{cases} \tag{24}$$

Integration of the equation (21), results equation (25):

$$p = \int_0^{\theta} [G_1(\theta)p + G_2(\theta) + G_3(\theta)] d\theta \tag{25}$$

Equation (25) is integrated using the trapezoidal rule.

Boundary conditions for entry and exit contact pressures are required. Boundary condition equations (26-28) are evaluated through infinitesimal equilibrium equations as well. Constant friction coefficient $\mu = 0.3$ is used in the ARCPRESS and the FE-model. Rolling pressure at the entrance $\theta = \alpha$ depending on frictional conditions is following:

if $\mu \cdot p_{en} > k_{en}$, sticking friction conditions, $\tau_{en} = k_{en}$:

$$p_{en} = 2k_{en} - \sigma_{tens\_en} - \sigma_{tens\_en} \cdot tan\,\alpha \tag{26}$$

if $\mu \cdot p_{en} \leq k_{en}$, slipping friction conditions, $\tau_{en} = \mu \cdot p_{en}$:

$$p_{en} = \frac{2k_{en} - \sigma_{tens\_en}}{1 + \mu \cdot tan\,\alpha} \tag{27}$$

Contact pressure at the exit point ($\theta = 0$) of the contact is:

$$p_{ex} = 2k_{ex} - \sigma_{tens\_ex} \tag{28}$$

With assumption of circular contact arc between WR and rolled material the equation (29) is used to calculate roll force per unit width. Roll force is calculated considering vertical components of contact pressure and frictional shear stresses [12]. Deformed WR radius *R'* is focused together with roll force *P* in the iteration process. Neutral angle β is defined in intersection point of contact pressure curves.

$$P = R' \int_0^{\alpha} p \cdot cos\left(\theta - \frac{1}{2}\alpha\right) d\theta + R' \left[\int_{\beta}^{\alpha} \tau \cdot sin\left(\theta - \frac{1}{2}\alpha\right) d\theta - \int_0^{\beta} \tau \cdot sin\left(\theta - \frac{1}{2}\alpha\right) d\theta\right] \tag{29}$$

4. Results

ACRPRESS setup calculations are automatically calculated for all six stands of finishing mill and sent forward for VUAMP-subroutine as initial rolling parameters. VRA use these predicted values at strip threading whereupon VRA receives measured data from FE-model. Predicted rolling pressure and friction shear stress distributions for two steel grades with different pass schedules are presented in figures 5 and 6. Sticking and slipping friction regions can be seen in friction shear stress distributions. True strain and flow stress evolution in roll gap for the first pass are also depicted in figures 5 and 6. Strain hardening is considerably high due to initial strain at entry plane in Hensel-Spittel was set 0.01 which corresponds to flow stress value of ~50 MPa for the used Hensel-Spittel fitting. At both cases contact pressure increases notable for next five passes. This can be explained by lower strip temperature, strain hardening, ratio of WR radius and strip thickness and partly with lack of recrystallization phenomena which are not considered in the model. Pass schedules used in figures 5 and 6 are shown in table 2.

Table 2. Pass schedules for ARCPRESS calculations.

Pass schedule 1	Pass	t_{en} [mm]	t_{ex} [mm]	T [°C]	w [mm]	R [mm]	$tens_{en}$ [MPa]	$tens_{ex}$ [MPa]
	1	38.94	29.23	922.0	1507.0	342.0	0.0	6.0
	2	29.23	22	Comp.*	1507.0	350.675	6.0	7.0
	3	22	17.26	Comp.*	1507.0	366.015	7.0	8.0
	4	17.26	14.66	Comp.*	1507.0	356.945	8.0	9.0
	5	14.66	13.07	Comp.*	1507.0	371.88	9.0	9.0
	6	13.07	12.27	Comp.*	1507.0	357.91	9.0	0.0
Pass schedule 2	Pass	t_{en} [mm]	t_{ex} [mm]	T [°C]	w [mm]	R [mm]	$tens_{en}$ [MPa]	$tens_{ex}$ [MPa]
	1	29.6	15.13	1030.0	1230.0	374.28	0.0	6.0
	2	15.13	7.69	Comp.*	1230.0	368.175	6.0	9.0

3	7.69	5.14	Comp.*	1230.0	350.225	9.0	11.0
4	5.14	3.86	Comp.*	1230.0	340.225	11.0	13.0
5	3.86	3.2	Comp.*	1230.0	369.645	13.0	16.0
6	3.2	2.83	Comp.*	1230.0	341.29	16.0	0.0

*Comp. = Computational

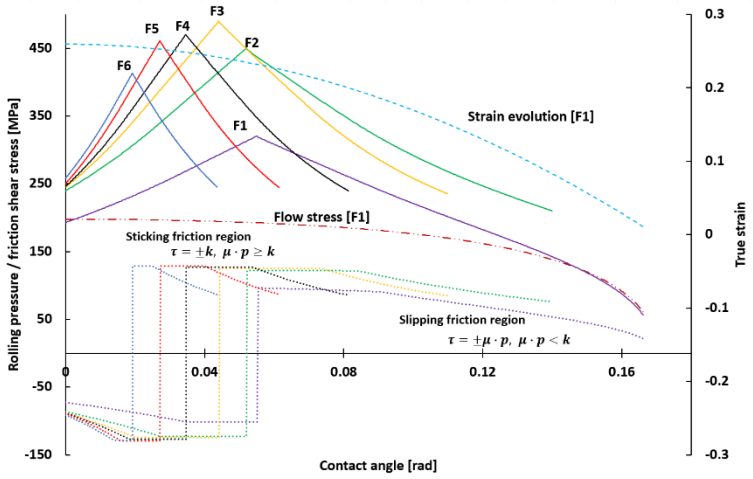

Figure 5. Contact pressure, friction shear stress, strain and flow stress evolution in roll gap with pass schedule 1.

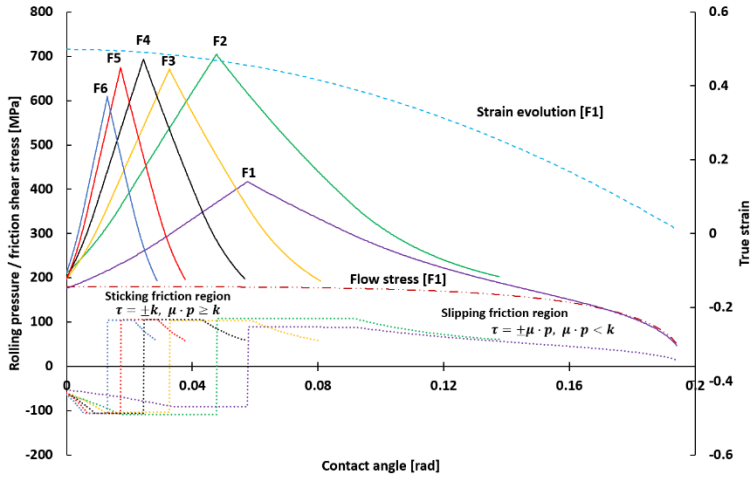

Figure 6. Contact pressure, friction shear stress, strain and flow stress evolution in roll gap with pass schedule 2.

4.1. Model verification

Theory and phenomena of the ARCPRESS model are verified utilizing computational results of formerly verified FE-model of finishing mill. Contact pressures CPRESS were collected to figure 7 from contact surfaces of the WR and the strip at first rolling stand. Element length on the contact surface of WR was 0.5 mm and the same initially in the strip. However, thickness reduction in the roll gap enforces longitudinal strain according to mass flow equilibrium leading a different size element length on contact surfaces. When surface elements remain almost equal dimensions the CPRESS curves are identical. Oscillation on the CPRESS distribution of the WR can be noticed when longitudinal strain on the surface of the strip is 0.4. At this point node points on contact surfaces are not eclipsed due to sliding and plastic

deformation in the strip. This seems to lead oscillation on the fully elastic WR but in proportion similar oscillation do not occur on the surface of the strip. Plastic properties of the strip may dampen oscillations of the strip. CPRESS curves are presented in cartesian coordinates in figure 7 and in cylindrical coordinates in figure 8.

Table 3. Rolling pass parameters for validation.

Pass parameters verification	Pass	t_{en} [mm]	t_{ex} [mm]	T [°C]	w [mm]	R [mm]	$tens_{en}$ [MPa]	$tens_{ex}$ [MPa]
	1	25.57	14.25	1027.7	1280.0	362.835	0.0	6.0

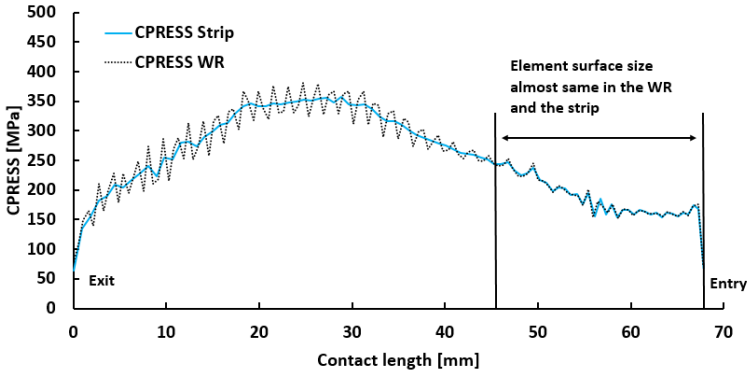

Figure 7. CPRESS distribution of strip and WR surfaces in FE-model.

Comparison between ARCPRESS contact pressure and friction shear stress distributions compared to CPRESS and CSHEAR of the FE-model is depicted in figure 8. ARCPRESS contact pressure is calculated by two or four separate functions depending on frictional conditions which intersect in neutral point, which is also known as friction hill. These functions always formulate a clear point of discontinuity at neutral point whereas FEM solution remain conformity. The greatest difference between these curves is located on neutral plane.

The comparison between the CSHEAR value obtained from the Abaqus FE model and the frictional shear stress obtained from the ARCPRESS analytical model does not show significant differences. Largest deviation between these curves is also near the neutral point. This can be explained similarly to the differences in contact pressures that were discussed earlier. In ARCPRESS calculation the direction of frictional shear is assumed to change direction in neutral point discontinuously, while in the FEM the change is continuous.

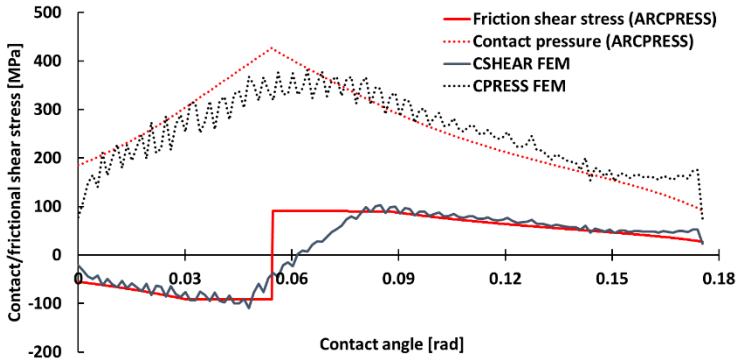

Figure 8. Comparison of CPRESS and CSHEAR distributions (FE) to contact pressure and friction shear stress (ARCPRESS).

5. Conclusion

ARCPRESS setup calculations for the FE-model of finishing mill is developed and implemented into virtual rolling automation in the FE-model. Initial rolling parameters are obtained from ARCPRESS calculations and utilized in pre-adjustment of the FE-model of finishing mill. Roll force prediction is based on calculations of contact pressure and friction shear stress distributions. Slipping and sticking zones are considered as well as strain hardening over the contact arc. Validation was carried out by comparing CPRESS and CSHEAR in the FE-model to contact pressure and friction shear stress distributions in ARCPRESS calculations. Results show very good agreement between the FE and ARCPRESS models.

Next step in further development of the ARCPRESS is calculation of absolute WR flattening. Accurate prediction of normal displacement of WR surface is critical for rolling automation system. To produce aimed exit thickness of the strip, enable stable rolling on next rolling stands. The current ARCPRESS model constructs the mechanical base for the virtual rolling model which is under development by authors.

References

[1] Hitchcock J 1935 Roll Neck Bearing, Appendix I *Am. Soc. Mech. Eng, New York* **286**
[2] Alexander J M and A P R S L 1972 On the theory of rolling *Proc. R. Soc. London. A. Math. Phys. Sci.* **326** 535–63
[3] Browne K M 1983 Modelling the thermophysical properties of iron and steels *Proceedings of Materials 98 – The Biennial Conference of the Institute of Materials Engineering* ed M Ferry pp 433–8
[4] Von Karman T 1925 Beitrag zur theorie des walzvorganges *Zeitschrift fur Angew. Math. und Mech.* **5** 139–41
[5] Orowan E 1943 The calculation of roll pressure in hot and cold flat rolling *Proc. Inst. Mech. Eng.* **150** 140–67
[6] Sims R B 1954 Calculation of roll force and torque in cold rolling by graphical and experimental methods *Iron Steel Inst.* **178** 19–34
[7] Bagheripoor M and Bisadi H 2013 Application of artificial neural networks for the prediction of roll force and roll torque in hot strip rolling process *Appl. Math. Model.* **37** 4593–607
[8] Li L, Xie H, Liu T, Huo M, Li X, Liu X, Wang E, Li J, Liu H, Sun L and others 2022 Numerical analysis of the strip crown inheritance in tandem cold rolling by a novel 3D multi-stand FE model *Int. J. Adv. Manuf. Technol.* **120** 3683–704
[9] Yildiz S K, Forbes J F, Huang B, Zhang Y, Wang F, Vaculik V and Dudzic M 2009 Dynamic modelling and simulation of a hot strip finishing mill *Appl. Math. Model.* **33** 3208–25
[10] Ilmola J, Seppälä O, Leinonen O, Pohjonen A, Larkiola J, Jokisaari J and Putaansuu E 2018 Multiphysical FE-analysis of a front-end bending phenomenon in a hot strip mill *AIP Conf. Proc.* **1960**
[11] Ilmola J, Pohjonen A, Seppälä O, Leinonen O, Larkiola J, Jokisaari J, Putaansuu E and Lehtikangas P 2018 Coupled multiscale and multiphysical analysis of hot steel strip mill and microstructure formation during water cooling *Procedia Manuf.* **15** 65–71
[12] Chen S, Li W and Liu X 2014 Calculation of rolling pressure distribution and force based on improved Karman equation for hot strip mill *Int. J. Mech. Sci.* **89** 256–63
[13] Freshwater I J 1996 Simplified theories of flat rolling - I. The calculation of roll pressure, roll force and roll torque Int. J. Mech. Sci. 38 633–48
[14] Freshwater I J 1996 Simplified theories of flat rolling - II. Comparison of calculated and experimental results *Int. J. Mech. Sci.* **38** 649–60
[15] Opěla P, Schindler I, Kawulok P, Vančura F, Kawulok R, Rusz S and Petrek T 2015 Hot flow stress models of the steel C45 *Metalurgija* **54** 469–72

[16] Ilmola J, Seppälä O, Leinonen O, Pohjonen A, Larkiola J, Jokisaari J and Putaansuu E 2018 Multiphysical FE-analysis of a front-end bending phenomenon in a hot strip mill *AIP Conference Proceedings* vol 1960
[17] Roberts W L 1983 *Hot rolling of steel* (Crc Press)

Acknowledgments
Financial assistance of the Business Finland, project FOSSA- Fossil-Free Steel Applications, is acknowledged. Likewise, the authors also acknowledge the valuable scientific and technical input and knowhow to the research by M.Sc. Juha Uusitalo, M.Sc. Jussi Paavola from the laboratory of Materials and Mechanical Engineering at the University of Oulu and thought-provoking conversations with M.Sc. Juha Pyykkönen from SSAB Europe.